J Fluoresc (2012) 22:111–119
DOI 10.1007/s10895-011-0936-x

ORIGINAL PAPER

Spectroscopic and Molecular Modeling Studies of the Interaction Between 4′-*O*-(α-L-Oleandrosyl)daunorubicin and Human Serum Albumin and Its Analytical Application

Ruina Huo · Cui Li · Fengling Cui · Guisheng Zhang · Qingfeng Liu · Xiaojun Yao

Received: 18 April 2011 / Accepted: 28 July 2011 / Published online: 4 August 2011

Abstract 4′-*O*-(α-L-Oleandrosyl)daunorubicin (ODNR) is a disaccharide analogue of daunorubicin with potent antitumor activity against leukemia cell line K562 cells and colon cancer cell line SW620 cells. In this paper, the binding interaction of ODNR with human serum albumin (HSA) was investigated under simulative physiological conditions by fluorescence spectroscopy in combination with UV absorption spectroscopy and molecular modeling method. A strong fluorescence quenching reaction of ODNR to HSA was observed and the quenching mechanism was suggested as static quenching according to the Stern-Volmer equation. The binding constants (K) at different temperatures as well as thermodynamic parameters, enthalpy change (ΔH) and entropy change (ΔS), were calculated according to relevant fluorescent data and Van't Hoff equation. The hydrophobic interaction was a predominant intermolecular force in order to stabilize the complex, which was in agreement with the results of molecular modeling study. In addition, the effects of other ions on the binding constants were also studied. Moreover, the synchronous fluorescence technique was successfully employed to determine the total proteins in serum, urine and saliva samples at room temperature under the optimum conditions with a wide linear range and satisfactory results.

Keywords 4′-*O*-(α-L-Oleandrosyl)daunorubicin · Human serum albumin · Fluorescence quenching · Molecular modeling · Synchronous fluorescence

R. Huo · F. Cui (✉) · G. Zhang (✉) · Q. Liu
School of Chemistry and Environmental Science,
Henan Normal University,
46 Jian-she Road,
Xinxiang 453007, People's Republic of China
e-mail: fenglingcui@hotmail.com
e-mail: zgs6668@yahoo.com

C. Li
School of Automation & Electrical Engineering,
University of Science and Technology Beijing,
Beijing 100083, People's Republic of China

X. Yao
Department of Chemistry, Lanzhou University,
Lanzhou 730000, People's Republic of China

Introduction

Anthracyclines are considered to be some of the most effective anticancer drugs for cancer therapy. However, drug resistance and cardiotoxicity of anthracyclines limit their clinical application. Many researchers have explored to modify the structure of anthracycline to generate more analogs to reduce the side effects and reverse multidrug resistance; however, these efforts only have limited success. Recently, G. Zhang et al. reported a novel class of disaccharide analogues of daunorubicin against leukemia cell line K562 cells and colon cancer cell line SW620 cells [1, 2]. In these disaccharide analogues, the first (inner) sugar in the carbohydrate chain is a daunosamine and the second sugars that linked to the first sugar are a series of uncommon sugars. Of all these disaccharide anthracyclines, the compounds with α-configuration of terminal 2,6-dideoxy sugar showed potent anticancer activities and higher topo II targetability, and at least 2–4 fold higher activity against drug-resistant cells than parent compound daunorubicin. They are worthy of further evaluation as new drug candidates. In this paper, we reported the investigation on the binding of the compound 4′-*O*-(α-L-oleandrosyl) daunorubicin (ODNR, Fig. 1), one disaccharide anthracy-

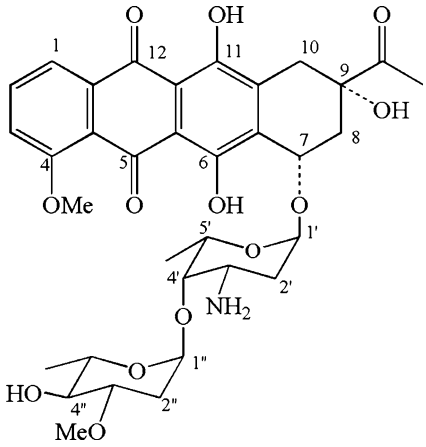

Fig. 1 The structural of ODNR

cline with α-configuration of terminal 2,6-dideoxy sugar (α-L-oleandrose), to human serum albumin (HSA).

HSA is a principle extracellular with a high concentration in blood plasma (40 mg/mL or 0.6 mmol) and serves as a protein storage component. Its three-dimensional structure has been determined through X-ray crystallographic measurements [3]. HSA is a globular protein composed of three structurally similar domains (I-III), each containing two subdomains (A and B) and is stabilized by 17 disulfide bridges [4]. It is the major transport protein for unesterified fatty acids, and is also capable of binding an extraordinarily diverse range of metabolites, drugs and organic compounds. The remarkable binding properties of albumin can play in both the efficacy and rate of delivery of drugs. Many drugs, including anticoagulants, tranquilizers, and general anesthetics [5, 6] are transported in the blood while bound to albumin. Up to now, extensive investigations into interactions between protein and internal compounds or pharmaceutical molecules have been stimulated [7–9]. This is because information concerning the interaction of serum albumin and a drug can help us to better understand the interaction mechanism and the absorption, as well as the distribution and toxicity of drugs. Molecular interactions are often monitored by optical techniques. These methods are sensitive and relative easy to use, whereas fluorescence spectroscopy is a valuable technique for studying interactions between small molecules and biomolecules, as well as inner ions. Information obtained concerning the emission wavelength, fluorescence polarization, energy transfer and fluorescence longevity is useful for analyzing the structure and site of the fluorophore in protein.

The determination of proteins is very important in clinical medicine, biochemistry, and laboratory tests. The most frequently used methods are Bromocresol Green (BCG) [10], Coomassie Brilliant Blue (CBB) [11], and Bromophenol Blue [12]. In recent years, novel methods such as electrochemistry technique [13], spectrofluorometry [14], Resonance Light Scattering (RLS) [15], and chemiluminescence [16] have been developed. Recently, synchronous fluorescence scan (SFS) analysis has become a new attractive method for the determination of biomolecules. The main characteristics of SFS are a narrowing of the spectral band, simplification of the emission spectra, and contraction of the spectral range. Because of its sharp and narrow spectrum, SFS serves as very simple, effective method of obtaining data for quantitative determination in a single measurement. Recently, there were some reports devoted to studies of the interaction between drugs and serum albumin [17, 18]. However, the interaction between ODNR and HSA, and the synchronous fluorescence determination of HSA have not been reported. Compared with other fluorescence probe reported, an obvious characteristic was that the binding mode was investigated by using molecular modeling, the sensitivity and selectivity were higher, the photostability was higher because the fluorescence intensity was basically kept at a constant value for at least 7 h, or there was a wider linear range.

In the present paper, the mechanism of interaction between ODNR and HSA has been studied using fluorescence spectroscopic technique and molecular modeling method under physiological condition. Spectroscopic data were used to quantify the binding constants of ODNR to HSA and the action distance which was based on the Förster's energy transference. Synchronous spectroscopy revealed that the change of protein structure resulted from the ODNR binding to several amino acids on the hydrophobic pocket of HSA. What is more, the interaction of the mainly acting forces and the binding site of the location were characterized by optical spectroscopy. Based on these results, a means of sensitive determination of protein was established. Detecting the protein in biology samples validates its reliability and its results were satisfactory.

Experimental

Materials

Appropriate amounts of human serum albumin (Hualan Biological Engineering Limited Company) were directly dissolved in water to prepare stock solution at final concentration of 2.0×10^{-5} mol/L and stored in the dark at 0~4 °C. 3.04×10^{-4} mol/L ODNR, 0.5 mol/L NaCl working solution, 0.1 mol/L Tris-HCl buffer solution of pH 7.4 and other ionic solutions were prepared. Human serum sample was obtained from the Hospital of Henan Normal University. The serum sample was diluted 100-fold with double water before determination. All chemicals were of analytical reagent grade and were used without further purification. Double distilled water was used throughout.

Apparatus

All fluorescence spectra were recorded on an FP-6200 spectrofluorimeter (JASCO, Japan) and a RF-540 spectrofluorimeter (Shimadzu, Japan) equipped with a thermostat bath, using 5 nm/5 nm slit widths. The UV absorption spectra were performed on a TU-1810 ultraviolet-visible spectrophotometer (Beijing General Instrument, China). The pH values were measured on a pH-3 digital pH-meter (Shanghai Lei Ci Device Works, Shanghai, China) with a combined glass electrode. All calculations were performed on SGI workstation while studying the molecular model.

Optimization of Experimental Conditions

In order to get the best results, the optimal conditions were investigated. Various experimental parameters including medium, pH, addition order, reaction temperature and $\Delta\lambda$ were studied with ODNR concentration being 3.04×10^{-6} mol/L in all conditions. The experimental results showed us that 0.1 mol/L Tris-HCl buffer solution of pH 7.4 was chosen as the supporting media; the Tris-HCl+NaCl+HSA+ODNR was selected in this work; 294 K was suggested as the preferable reaction temperature.

Measurements of Spectrum

Under the optimum physiological conditions described above, 2.0 mL Tris-HCl buffer solution, 2.0 mL NaCl solution, appropriate amounts of HSA and ODNR were added to 10.0 mL standard flasks and diluted to 10.0 mL with double distilled water. Fluorescence quenching spectra of HSA were obtained at excitation wavelength (280 nm) and emission wavelength (300~450 nm). Fluorescence spectra in the presence of other ions were also measured at the same conditions. In addition, molecular modeling and synchronous fluorescence spectra of system were recorded.

Protein-Ligand Docking Study

The potential of the 3D structure of HSA was assigned according to the Amber 4.0 force field with Kollman-all-atom charges. The initial structures of all the molecules were generated by molecular modeling software Sybyl 6.9 [19]. The geometries of this drug were subsequently optimized using the Tripos force field with Gasteiger-Marsili charges. FlexX program was applied to calculate the possible conformation of the drug that binds to the protein. The crystal structure of HSA in complex with R-warfarin was taken from the Brookhaven Protein Data Bank (entry codes 1h9z). The PDB file contains a co-crystal with a small ligand (R-warfarin) in the active site. This ligand was extracted and used as a reference structure (a fixed conformation docked into the active site of the HSA). FlexX program used the reference structure for the active site determination by default, any residue in the protein within 6.5Å of the reference structure was considered part of the active site. FlexX program also did an RMS comparison between the reference structure and final docked structure of ODNR as an indication of accuracy. The receptor descriptor file (rdf) lies at the heart of FlexX. It contains the information about the protein, its amino acids, the active site, non-amino acid residues, and specific torsion angles. Sybyl interface to FlexX created a default-rdf file. At last, FlexX program was used to build the interaction modes between the ODNR and HSA. ODNR was docked to HSA by FlexX and then it revealed hydrogen bonds between ODNR and some residues of HSA. All calculations were performed through SGI FUEL workstations.

Results and Discussion

Fluorescence Quenching Mechanism and Binding Constants

To investigate whether ODNR binds to HSA, fluorescence measurements were carried out, which could give informations about the molecular environment in a vicinity of the chromophore molecules. Figure 2 shows the fluorescence emission spectra of HSA in the absence and presence of ODNR in the range of 300~450 nm upon excitation 280 nm. The fluorescence intensity of HSA decreased regularly with increasing concentration of ODNR and the maximum emission wavelength exhibits hypsochromic shift if the concentration of HSA was fixed, indicating that

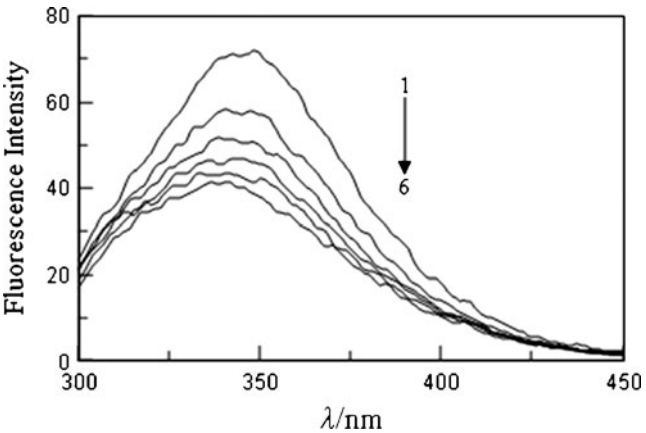

Fig. 2 The fluorescence spectra of ODNR-HSA system. From 1 to 6: $C_{HSA}=1.2\times10^{-6}$ mol/L; $C_{ODNR}=0$, 3.04, 6.08, 9.12, 12.16, 15.20×10^{-6} mol/L

ODNR had a strong ability to quench fluorescence of HSA, and the binding of ODNR to HSA altered the polarity of the local dielectric environment.

For reconfirming the structural change of HSA by addition of ODNR, we measured the UV absorbance spectra of HSA with various amounts of ODNR. Figure 3 displays the UV absorbance spectra of HSA in the absence and presence of ODNR. As can be seen in Fig. 3, HSA has strong absorbance with a peak at 230 nm and the absorbance of HSA increased with the addition of ODNR and toward longer wavelength; the chromophore of ODNR gives a very specific pattern of the UV spectrum with slight dual absorbance at higher concentration of ODNR in the system from 251 to 289 nm. The obvious enhancement of UV absorbency intensity (A) and the change of absorption spectra verified the formation of a new complex between ODNR and HSA. Thus, the evidences from fluorescence and UV spectra indicated that the interaction of ODNR and HSA bring about the microenvironment change around HSA.

The differentiation of static quenching and dynamic quenching could be shown from quenching rate constant at different temperatures. The quenching rate constant decreased with increasing temperature for static quenching, while the reversed effect would be observed for the dynamic quenching [20]. The possible quenching mechanism could be interpreted by fluorescence quenching spectra of the protein and the F_0/F-C (Stern-Volmer) curves of HSA with ODNR at different temperatures (294, 304, 314 K) were shown in Fig. 4.

It could be found from Fig. 4 that the Stern-Volmer plots were linear and the slopes decreased when temperature rose, indicating that it was static quenching interaction

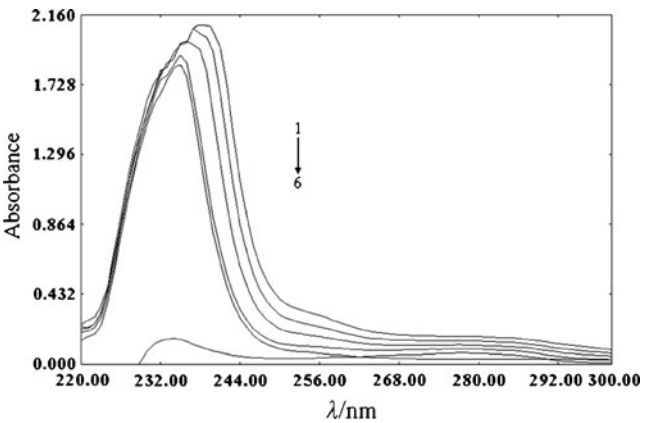

Fig. 3 UV absorption spectra of HSA in the absence and presence of ODNR. (1–4) The UV absorption of ODNR-HSA, $C_{HSA}=8\times10^{-7}$ mol/L; $C_{ODNR}=12.16\times10^{-6}$ mol/L, $C_{ODNR}=9.12\times10^{-6}$ mol/L, $C_{ODNR}=6.08\times10^{-6}$ mol/L, $C_{ODNR}=3.04\times10^{-6}$ mol/L; (5) The UV absorption of HSA, $C_{HSA}=8\times10^{-7}$ mol/L; (6) The UV absorption of ODNR, $C_{ODNR}=3.04\times10^{-6}$ mol/L

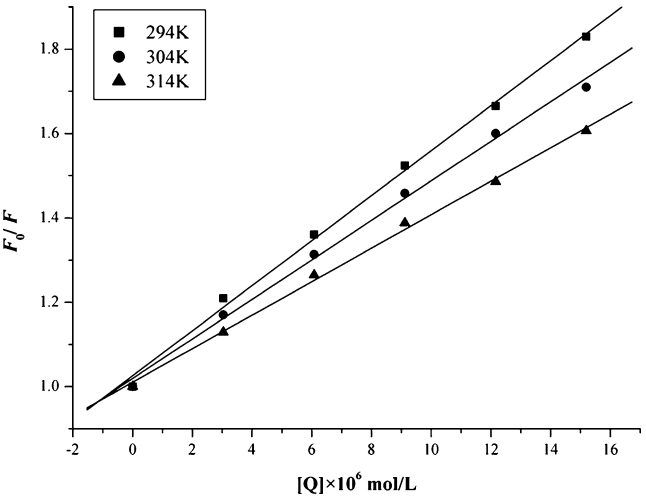

Fig. 4 The Stern-Volmer curves for quenching of ODNR with HSA

between ODNR and HSA. In order to confirm this view, the procedure was assumed to be dynamic quenching. The quenching equation is [21]:

$$F_0/F = 1 + K_q\tau_0[Q] = 1 + K_{sv}[Q] \quad (1)$$

Where F_0 and F are initial and current fluorescence intensity of biomolecule, respectively. K_q, K_{sv}, τ_0 and $[Q]$ represent the quenching rate constant of the biomolecule, the Stern-Volmer quenching constant, the average lifetime of molecule without quencher and concentration of quencher, respectively. Because the fluorescence lifetime of the biopolymer is 10^{-8} s [22], K_{sv} is the slope of linear regressions of Fig. 4. According to Eq. 1, the quenching constant K_q could be calculated and are listed in Table 1 together with the correlation coefficients. However, the maximum scatter collision quenching constant of various quenchers with the biopolymer is 2.0×10^{10} J/mol/K [23]. Obviously, the rate constant of protein quenching procedure initiated by ODNR was greater than the K_q of the scatter procedure. Therefore, the quenching was not initiated by dynamic collision but from new compound formation. In Fig. 3, the change of peak before and after the addition of ODNR can testify the formation of new complex in combination with obvious enhancement of absorbency intensity (A). Therefore, the quenching of HSA fluorescence by ODNR depended on the formation

Table 1 The dynamic quenching constants (L/mol/s) between ODNR and HSA

T(K)	Stern-Volmer equation	K_q (L/mol/S)	R
294	$Y=1.026+5.334\times10^4$ [Q]	5.334×10^{12}	0.9984
304	$Y=1.019+4.686\times10^4$ [Q]	4.686×10^{12}	0.9982
314	$Y=1.010+3.971\times10^4$ [Q]	3.971×10^{12}	0.9988

of the new complex of ODNR and HSA. The static quenching equation was presented by [24]:

$$(F_0 - F)^{-1} = F_0{}^{-1} + K^{-1}F_0{}^{-1}[Q]^{-1} \quad (2)$$

Where K denotes the binding constant of ODNR and biomolecule, which could be calculated from the slope and intercept of Lineweaver-Burk curves as shown in Fig. 5 (K=intercept/slope). The results are listed in Table 2. It could be found that there was a strong interaction between ODNR and HSA. The interaction was weakened when the temperature rose, but the effect of temperature was small. Thus, the quenching efficiency of ODNR to HSA was not obviously reduced when the experimental temperature increased.

The Determination of Binding Mode

Considering the dependence of binding constant on temperature, a thermodynamic process was considered to be responsible for the formation of the complex. Therefore, the thermodynamic parameters dependent on the temperatures were analyzed in order to characterize the acting forces between ODNR and HSA. The acting forces between a small molecule substance and macromolecule mainly include hydrogen bond, van der Waals force, electrostatic force, hydrophobic interaction force, and so on. The thermodynamic parameters, enthalpy (ΔH), entropy (ΔS) and free energy change (ΔG), are mainly evidence to estimate the binding mode. The thermodynamic parameters were evaluated from the following equations [25]:

$$\ln K = -\Delta H/RT + \Delta S/R \quad (3)$$

$$\Delta G = \Delta H - T\Delta S = -RT\ln K \quad (4)$$

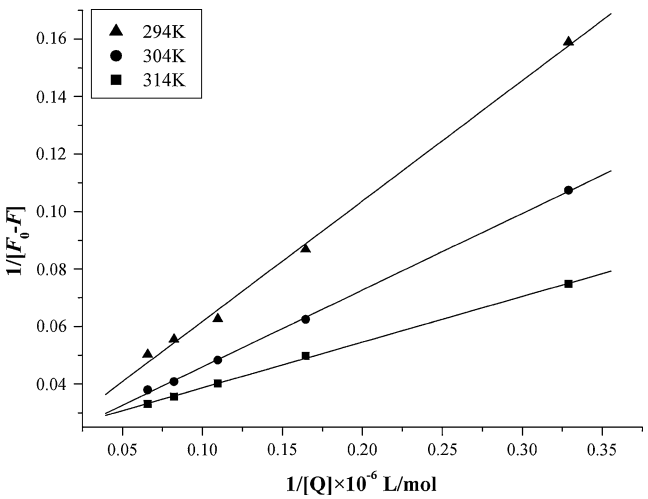

Fig. 5 The Lineweaver-Burk curves for quenching of ODNR with HSA

Table 2 The binding constants (L/mol) between ODNR and HSA at different temperatures

T (K)	Lineweaver-Burk equation	K (L/mol)	R
294	$Y=0.02281+0.1588\times10^{-6}$ 1/[Q]	1.44×10^5	0.9985
304	$Y=0.01925+0.2670\times10^{-6}$ 1/[Q]	9.89×10^4	0.9997
314	$Y=0.01907+0.4191\times10^{-6}$ 1/[Q]	6.95×10^4	0.9996

where ΔH, ΔG and ΔS are, respectively, enthalpy change, free energy change and entropy change; R is the gas constant. ΔH and ΔS for the binding reaction of ODNR and HSA were calculated to be −17.97 kJ/mol and 36.52 J/mol/K, respectively; at 294, 304 and 314 K, ΔG calculated were −29.03, −29.07 and −29.11 kJ/mol, respectively. Indicating that the formation of ODNR-HSA coordination compound was spontaneous and exothermic reaction accompanied a positive ΔS value. According to the views of Neméthy and Scheraga [26], Ross and Subramananian [27], the positive ΔS value is frequently taken as evidence for hydrophobic interaction. Furthermore, specific electrostatic interactions between ionic species in aqueous solution are characterized by a positive value of ΔS and a negative ΔH value. Accordingly, it was not possible to account for the thermodynamic parameters of ODNR-HSA compound on the basis of a single interaction molecular force model. It was more likely that hydrophobic and electrostatic interactions were involved in the binding process. But ODNR might be considered to be largely unionized under the experimental conditions, as can be expected from its structure. Hence, electrostatic interaction can be precluded from the binding process. Thus, ODNR bound to HSA was mainly based on the hydrophobic interaction.

Molecular Modeling Study of the Interaction between ODNR and HSA

The application of molecular modeling by computer methods has been employed to improve the understanding of the interaction of ODNR and HSA. Descriptions of 3D structure of crystalline albumin have revealed that HSA comprises of three homologous domains that assemble to form a heart-shaped molecule. HSA is monomeric but contains the three structurally similar α-helical domains (I-III); each domain has two subdomains (A and B), which are six (A) and four (B) α-helices, respectively. The principal regions of ligand binding to HSA are located in hydrophobic cavities in subdomains IIA and IIIA, which are consistent with site I and site II, respectively, and one tryptophan residue (Trp-214) of HSA is in subdomain IIA. Several studies have shown that HSA is able to bind many ligands in several

binding sites [28]. The crystal structure of HSA in complex with R-warfarin was taken from the Brookhaven Protein Data Bank (entry codes 1h9z). The potential of the 3D structure of HSA was assigned according the Amber 4.0 force field with Kollman-all-atom charges. The initial structure of all the molecules was generated by molecular modeling software Sybyl 6.9 [19]. The geometries of these compounds were subsequently optimized using the Tripos force field with Gasteiger-Marsili charges. FlexX program was applied to calculate the possible conformation of the ligands that binds to the protein. The conformer with RMS (root-means-square) was used for further analysis. Based on this kind of approach a computational model of the target receptor has been built, partial binding parameters of the ODNR-HSA system were calculated through SGI FUEL workstations. The best energy ranked results of the binding mode between ODNR and HSA is shown in Fig. 6, as shown in Fig. 6, ODNR binds within the subdomain IIA of the protein (The Warfarin Binding Pocket). The ODNR moiety is located within the binding pocket. It is important to note that the residue Trp-214 of HSA is in close proximity to the ODNR molecular suggesting the existence of hydrophobic interaction between them. On the other hand, there are hydrogen bonds between Arg218 and 5-O of ODNR molecule, Arg222 and 5-O, Arg222 and 6-O, Ala291 and H (6-OH of ODNR molecule), Glu292 and H (3′-NH_2 of ODNR molecule). The results indicated that the formation of hydrogen bond decreased the hydrophilicity and increase the hydrophobicity to stability the ODNR-HSA system. The amino acid residues with benzene ring can match that of the ODNR in space in order to firm the conformation of the complex. But the interaction between ODNR and HSA is not exclusively hydrophobic in nature since there are several polar residues in the proximity of the bound ligand (shown in arrows), which play a subordinate role in stabilizing the drug molecule via electrostatic interaction, which is also in agreement with the binding mode study. However, the results obtained from modeling indicated that the interaction between ODNR and HSA is dominated by hydrophobic force, and there are also hydrogen bonds between the drug and HSA. As compared to other small molecules with the similar structure on non-covalent binding of serum albumin previously reported, the value of the binding constant for ODNR was relatively large [29, 30]. It can be seen from Fig. 6 that this may because that more atoms are in the plan of the ring, thus less steric hindrance would be involved in the binding process. As a result, the binding of ODNR to HSA became easier relatively.

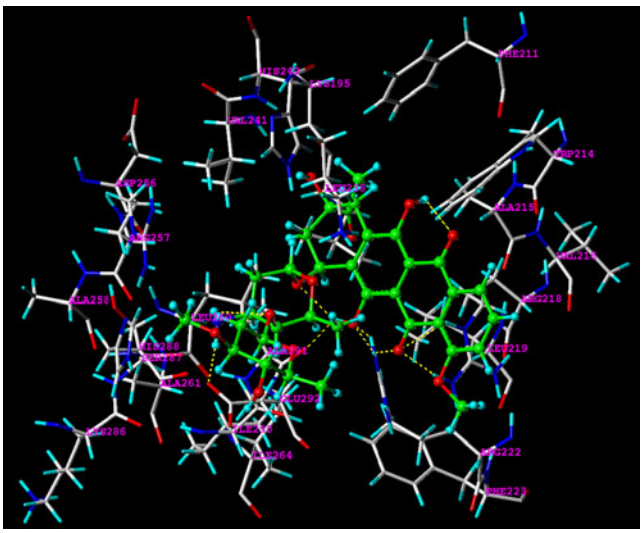

Fig. 6 The interaction model between ODNR and HSA. The residues of ODNR and HSA are represented using different tinctorial stick model. The hydrogen bond between the ligand and the protein is indicated by dashed line

The Energy Transfer Between ODNR and HSA

According to the Förster's theory [31], the efficiency of energy transfer is related to not only the distance between tryptophan residue (donor) and ODNR (acceptor), but also to the critical energy transfer distance. That is:

$$E = 1 - F/F_0 = R_0{}^6/\left(R_0{}^6 + r^6\right) \tag{5}$$

Where r represents the distance between donor and acceptor. R_0 is the critical distance when transfer efficiency is 50%, which can be calculated by

$$R_0 = 8.8 \times 10^{-25} k^2 n^{-4} \Phi J \tag{6}$$

Where k^2 is the orientation factor related to the geometry of the donor-acceptor of dipole, n is the refractive index of medium, Φ is the fluorescence quantum yield of the donor, J is the spectra overlap of the donor emission and the acceptor absorption. J is given by

$$J = \sum F(\lambda)\varepsilon(\lambda)\lambda^4 \Delta\lambda / \sum F(\lambda)\Delta\lambda \tag{7}$$

Where $F(\lambda)$ is the fluorescence intensity of the fluorescence reagent when wavelength is λ, $\varepsilon(\lambda)$ is the molar absorbance coefficient of the acceptor at the wavelength of λ. From these equations, J, E and R_0 can be calculated, so the value of r also can be evaluated. The overlap of the fluorescence spectrum of HSA and the absorption spectrum of ODNR is shown in Fig. 7.

From Fig. 7, the overlap integral calculated according to the above relationship were 2.12×10^{-14} cm^3·L/mol. It had been reported that: k^2=2/3, n=1.336, Φ=0.118 for HSA [32]. Based on these data, the distance between ODNR and tryptophan residue in HSA was 3.32 nm. Obviously, it was lower than 7 nm after interaction, which accorded with

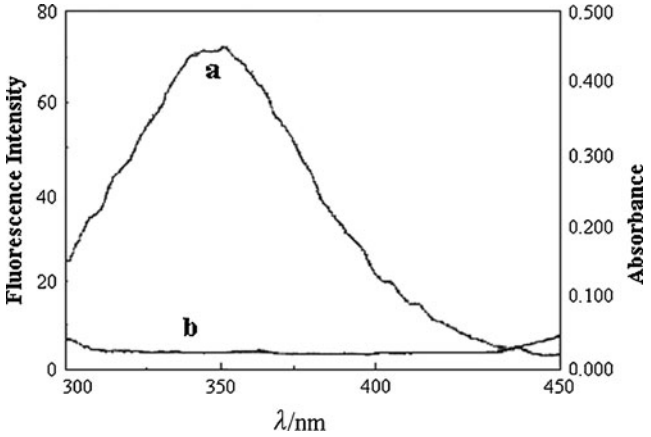

Fig. 7 The overlap of UV absorption spectrum of ODNR with the fluorescence spectrum of HSA. **a** The fluorescence spectrum of HSA (8×10^{-7} mol/L); **b** The UV absorption spectrum of ODNR (3.04×10^{-6} mol/L)

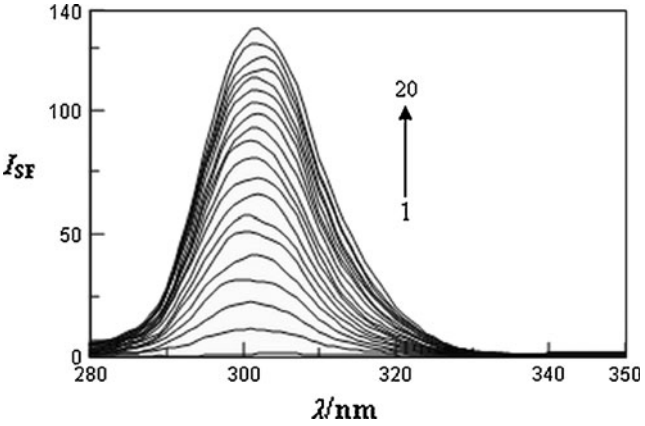

Fig. 8 Synchronous fluorescence spectra of ODNR with HSA. C_{ODNR}= 3.04×10^{-6} mol/L; from 1–20, C_{HSA}=0, 0.4, 0.8, 1.2, 1.6, 2.0, 2.4, 2.8, 3.2, 3.6, 4.0, 4.4, 4.8, 5.2, 5.6, 6.0, 6.4, 6.8, 7.2, 7.6×10^{-6} mol/L

conditions of Förster's non-radiative energy transfer theory, indicating that the energy transfer happened when binding between ODNR and HSA, and energy transfer might depend on the distance between the tryptophan residue and ODNR bound to HSA.

Effect of Other Ions on Binding Constants

The molecule of protein contains the elements of C, H, O, N, S and P. In addition, some of trace metal ions exist in the organism, and which has definite ability to bind proteins [33, 34]. To investigate the effect of coexistent ions, the binding constants in the presence of other ions were investigated at 294 K under the experimental conditions. The results are listed in Table 3. It showed that the binding constants between HSA and ODNR decreased in the presence of other ions, implying there was a binding between metal ions and HSA and the presence of metal ions directly affected the binding between ODNR and HSA. The competition between metal ions and ODNR decreased the binding constant between ODNR and HSA, implying that the binding force between ODNR and HSA also decreased, which caused the shortening of the storage time of ODNR in the blood plasma and enhancing the maximum effectiveness of ODNR.

Table 3 The binding constants between ODNR and HSA in the presence of other ions

Ions	K (10^4)	R	Ions	K (10^4)	R
SO_4^{2-}	14.10	0.9995	Pb^{2+}	12.62	0.9985
Zn^{2+}	8.088	0.9990	Mn^{2+}	12.30	0.9993
F^-	11.50	0.9990	Cd^{2+}	10.24	0.9988
Cu^{2+}	13.86	0.9985	NH_4^+	13.36	0.9972
Ca^{2+}	5.287	0.9991	Ni^+	9.875	0.9998
Hg^{2+}	7.783	0.9993	K^+	2.590	0.9992

Determination of HSA in Biology Samples

Precision, Limits of Detection and Working Curve

Based on the binding of HSA to ODNR, we employed synchronous fluorescence spectra to quantitative determine the human serum albumin. Figure 8 shows the synchronous spectra of HSA in the presence of appropriate ODNR. It could be seen that the synchronous fluorescence intensity (I_{SF}) of ODNR was very weak, so that the effect of ODNR on the determination of HSA could be eliminated, and the intensity of the synchronous fluorescence increased noticeably with increasing of the concentration of HSA. The enhancement intensity of synchronous fluorescence was

Table 4 Determination result of serum, urine and saliva samples (n=6)

Samples	Added/μg/mL	Found/μg/mL	Recovery/%	RSD/%
Serum	0	32.54		0.85
	55.20	90.28	104.6	1.01
	110.4	142.8	99.87	0.78
	165.6	198.87	100.5	0.56
Saliva	0	11.42		1.09
	55.2	65.46	97.90	0.43
	110.4	126.8	104.5	0.39
	165.6	178.4	100.8	0.96
Urine	0	20.64		0.79
	55.2	78.50	104.8	1.15
	110.4	129.6	98.70	0.83
	165.6	186.8	100.3	0.79

proportion to the concentration of HSA. The linear range determined was 1.660~552.0 μg/mL, the linear regression equations was $I_{HSA}=6.744+1.390\times10^{15}\ C_{HSA}$ (μg/mL) with a correlation coefficient (*R*) of 0.9984. The detection limit for HSA as defined by IUPAC was determined to be 1.28 μg/mL [35]. The relative standard deviation (*RSD*) was 1.26% for HSA, as obtained from 6 replicate determinations of 3.04×10^{-6} mol/L for ODNR.

Analysis of Biology Samples

Because the present method showed protein specificity, we thought it suitable for determining the total content of protein in complex samples containing different types of proteins (e.g.: serum albumin). Thus, this method was applied to the determination of total protein in serum, urine, saliva samples. Standard human serum, which was used to construct a calibration curve, was obtained by mixing 40 normal serum samples. Construction of the calibration curve and analysis of the serum, urine, saliva samples were then performed according to the procedures described above. Serum sample was diluted 100-fold with double distilled water just before determination without any other pretreatment, urine and saliva samples were also diluted appropriate folds. Table 4 displayed the results of determination by a standard addition method for biology samples, which were very satisfying. Therefore, the proposed method has potential for the sensitive and rapid determination of total protein in biology samples.

Conclusions

The interaction between ODNR and HSA has been investigated by different spectroscopy techniques under simulative physiological conditions. This study showed that the intrinsic fluorescence of HSA was quenched through static quenching mechanism and the binding of ODNR to HSA was predominantly owing to hydrophobic interaction estimated from the signs of ΔH and ΔS, which was consistent with the result from molecular modeling study. Experimental results showed that the binding of ODNR to HSA induced a conformational change of HSA, which was proved by the qualitative analysis data of UV absorbance. This study also showed that ODNR was a strong quencher and bound to HSA with high affinity. Based on this phenomenon, a new method by synchronous fluorescence for the rapid and simple determination of the proteins in biology samples was provided. The results showed that the present method was comparable with other methods in terms of sensitivity, rapid, simplicity and linear range. This method might be expanded to the application in biochemistry and clinic practice.

Acknowledgement This work was supported by the National Natural Science Foundation of China (grant numbers 30970696, 20872029).

References

1. Zhang GS, Fang LY, Zhu LZ, Aimiuwu JE, Shen J, Cheng H, Muller MT, Lee GE, Sun DX, Wang PG (2005) Syntheses and biological activities of disaccharide daunorubicins. J Med Chem 48:5269–5278
2. Battisti RF, Zhong YQ, Fang LY, Gibbs S, Shen J, Nadas J, Zhang GS, Sun DX (2007) Modifying the sugar moieties of daunorubicin overcomes p-gp-mediated multidrug resistance. Mol Pharm 4:140–153
3. He XM, Carter DC (1992) Atomic structure and chemistry of human serum albumin. Nature 358:209–215
4. Curry S, Brick P, Franks NP (1999) Fatty acid binding to human serum albumin: new insights from crystallographic studies. Biochim Biophys Acta 1441:131–140
5. Zilberman G, Smith AL (2005) QCM/HCC as a platform for detecting the binding of warfarin to an immobilized film of human serum albumin. Analyst 130:1483–1489
6. Sawas AH, Pentyala SN, Rebecchi MJ (2004) Binding of volatile anesthetics to serum albumin: measurements of enthalpy and solvent contributions. Biochemistry 43:12675–12685
7. Xu C, Zhang AP, Liu WP (2007) Binding of phenthoate to bovine serum albumin and reduced inhibition on acetylcholinesterase. Pestic Biochem Physiol 88:176–180
8. Wei YL, Li JQ, Dong C, Shuang SM, Liu DS, Huie CW (2006) Investigation of the association behaviors between biliverdin and bovine serum albumin by fluorescence spectroscopy. Talanta 70:377–382
9. Seedher N, Bhatia S (2006) Reversible binding of celecoxib and valdecoxib with human serum albumin using fluorescence spectroscopic technique. Pharm Res 54:77–84
10. Wei YJ, Li KA, Tong SY (1996) The interaction of Bromophenol Blue with proteins in acidic solution. Talanta 43:1–10
11. Bradford MM (1976) A rapid and sensitive method for the quantitation of microgram of protein utilizing the principle of protein-dye binding. Anal Biochem 72:248–254
12. Flores R (1978) A rapid and reproducible assay for quantitative estimation of proteins using bromophenol blue. Anal Biochem 88:605–611
13. Long JS, Silvester DS, Wildgoose GG, Surkus A-E, Flechsig G-U, Compton RG (2008) Direct electrochemistry of horseradish peroxidase immobilized in a Chitosan-[C_4mim][BF_4] film: Determination of electrode kinetic parameters. Bioelectrochemistry 74:183–187
14. Jiang CQ, Luo L (2004) Spectrofluorimetric determination of human serum albumin using a doxycycline-europium probe. Anal Chim Acta 506:171–175
15. Huang CZ, Li YF, Feng P (2001) Determination of proteins with α, β, γ, δ-tetrakis(4-sulfophenyl)porphine by measuring the enhanced resonance light scattering at the air/liquid interface. Anal Chim Acta 443:73–80
16. Li ZP, Fan SS, Zhang LN, Wang FC (2004) Time-resolved chemiluminescence technique for the microdetermination of proteins based on their complexation with copper(II). Anal Sci 20:1327–1331
17. Cui FL, Qin LX, Zhang GS, Yao XJ, Du J (2008) Binding of daunorubicin to human serum albumin using molecular modeling and its analytical application. Int J Biol Macromol 42:221–228

18. Meierhofer T, van den Elsen JMH, Cameron PJ, Muñoz-Berbel X, Jenkins ATA (2010) The interaction of serum albumin with cholesterol containing lipid vesicles. J Fluoresc 20:371–376
19. SYBYL Software, Version 6.9 (2002) Tripos Associates Inc., St. Louis, p. 584
20. Eftink MR (1991) Fluorescence quenching reaction: probing biological macromolecular structures, biophysical and biochemical aspects of fluorescence spectroscopy. Plenum, New York
21. Tian JN, Liu JQ, He WY, Hu ZD, Yao XJ, Chen XG (2004) Probing the binding of scutellarin to human serum albumin by circular dichroism, fluorescence spectroscopy, FTIR, and molecular modeling method. Biomacromolecules 5:1956–1961
22. Lakowicz JR, Weber G (1973) Quenching of fluorescence by oxygen. A probe for structural fluctuations in macromolecules. Biochemistry 12:4161–4170
23. Ware WR (1962) Oxygen quenching of fluorescence in solution: an experimental study of diffusion process. J Phys Chem 66:455–458
24. Tian JN, Liu JQ, Zhang JY, Hu ZD, Chen XG (2003) Fluorescence studies on the interactions of barbaloin with bovine serum albumin. Chem Pharm Bull 51:579–582
25. Song SM, Hou XL, Wu YB, Shuang SM, Yang C, Inoue Y, Dong C (2009) Study on the interaction between methyl blue and human serum albumin by fluorescence spectrometry. J Lumin 129:169–175
26. Némethy G, Scheraga HA (1962) The structure of water and hydrophobic bonding in proteins. III. The thermodynamic properties of hydrophobic bonds in proteins. J Phys Chem 66:1773–1789
27. Ross PD, Subramanian S (1981) Thermodynamics of protein association reactions: forces contributing to stability. Biochemistry 20:3096–3102
28. Kragh-Hansen U (1981) Molecular aspect of ligand binding to serum albumin. Pharmacol Rev 33:17–53
29. Bi SY, Ding L, Tian Y, Song DQ, Zhou X, Liu X, Zhang HQ (2004) Investigation of the interaction between flavonoids and human serum albumin. J Mol Struct 703:37–45
30. Sengupta B, Banerjee A, Sengupta PK (2005) Interactions of the plant flavonoid fisetin with macromolecular targets: Insights from fluorescence spectroscopic studies. J Photochem Photobiol B 80:79–86
31. Förster T (1996) In: Sinanoglu O (ed) Modern quantum chemistry, vol 3. Academic, New York
32. Cui FL, Fan J, Ma DL, Liu MC, Chen XG, Hu ZD (2003) A study of the interaction between a new reagent and serum albumin by fluorescence spectroscopy. Anal Lett 36:2151–2166
33. Emiko O, Yoshito H, Kana N, Susumu K (1999) The interaction between human and bovine serum albumin and zinc studied by a competitive spectrophotometry. J Inorg Biochem 75:213–218
34. Liang H, Huang J, Tu CQ, Zhang M, Zhou YQ, Shen PW (2001) The subsequent effect of interaction between Co^{2+} and human serum albumin or bovine serum albumin. J Ingor Biochem 85:167–171
35. Irving HMHN, Freiser H (1987) In: West TS (ed) IUPAC, Compendium of analytical nomenclature, definitive rules. Pergamon, Oxford